

## C1.1 New Data / Ozone (Terra)

### Ozone Data Assimilation System in Support of Terra Launch

The ozone is included as a new input data type to and as a new assimilated output field from the GEOS ozone DAS component of the Terra System. A global three-dimensional ozone field is produced by assimilation of the total column ozone observations from the Total Ozone Mapping Spectrometer (TOMS) (McPeters *et al.* 1998) and partial ozone profile observations from the Solar Backscatter Ultraviolet/2 (SBUV/2) instrument (Bhartia *et al.* 1996). The assimilating model is an off-line ozone transport forecast model (Lin and Rood 1996) that is driven by GEOS-3 assimilated winds. The assimilation is done using a global physical space based statistical analysis scheme (Cohn *et al.* 1998). The initial version of GEOS ozone DAS is described by Riishøjgaard *et al.* (1999). The current version of GEOS ozone DAS that is implemented as a component of the Terra System is described in detail by Štajner *et al.* (1999a), which is included as the next section C1.2 of this document. Alternative configurations of the GEOS ozone DAS that would be used in case of failure of either TOMS or SBUV instruments were identified and the assimilated fields produced using these configurations were validated by Štajner *et al.* (1999b). The following sections contain a brief description and examples from validation of the configuration of the GEOS ozone DAS being used for Terra support.

#### Description of GEOS ozone DAS

In the GEOS ozone DAS the forecast step consists of integrating the constituent advection equation

$$\frac{\partial \mu}{\partial t} + \mathbf{v} \cdot \nabla \mu = 0 \quad (1)$$

where  $\mu$  is the ozone mixing ratio and  $\mathbf{v}$  is the wind. A flux-form semi-Lagrangian advection scheme (Lin and Rood 1996) with a time step of 15 minutes is used to integrate this equation. In the current ozone assimilation system the chemical source and sink terms are not included. This decision was based on experiments using parameterized chemistry as in Riishøjgaard *et al.* (1999). The known bias between the source and sink terms and the observations was found to be substantial, leaving residual errors in the assimilated data product that were larger than those from the exclusion of chemistry. Effectively, since the time between different introductions of data into the system is small, the observations themselves are acting as the source and sink terms. Further since the bulk of the column resides in the lower stratosphere where the ozone is quasi-conservative, the ozone variability is dominated by advective processes. A notable shortcoming of neglecting the chemical terms is the ozone hole region. We expect to improve the representation of chemical processes with further study.

The SBUV profile data from Umkehr layer 3 and above (above 126 hPa) are assimilated together with TOMS total column ozone data. Both instruments are on board polar orbiting satellites.

The TOMS provides almost global coverage of the sunlit portion of the Earth in 24 hours. The SBUV instrument makes measurements at nadir only, also using the back-scattered sunlight. The SBUV data has vertical resolution of about 5 km, and horizontal resolution of about  $200 \times 200$  km. The horizontal resolution of TOMS is higher, varying from about  $40 \times 40$  km at nadir to about  $100 \times 100$  km at largest scan angles. Thus, prior to assimilation the TOMS data are averaged into  $2^\circ$  latitude by  $2.5^\circ$  longitude bins, which is the horizontal resolution of the forecast model. Consequently, about 10000 TOMS data in addition to about 1000 SBUV profiles are assimilated daily.

Assimilation of available observations is done after every model time step (15 minutes). The forecast vector  $\mu^f$  obtained by integrating eq. (1) is combined with the vector of ozone observations  $\tau^o$  to provide the best estimate or analysis of ozone  $\mu^a$  using the following statistical analysis equations. The innovation equation is solved for vector  $x$

$$(H P^f H^T + R) x = \tau^o - H \mu^f, \quad (2)$$

where  $H$  is the matrix of the observation operator, while  $P^f$  and  $R$  are forecast and observation error covariance matrices. The analyzed state  $\mu^a$  is obtained using the following equation

$$\mu^a = \mu^f + P^f H^T x. \quad (3)$$

The models that are used for  $P^f$ ,  $R$  and  $H$  are given and discussed in detail by Štajner *et al.* (1999a). The matrix  $R$  is diagonal except that the errors of the SBUV observations that belong to a single profile are modeled as correlated. The forecast error variance is modeled proportional to the forecast field. The horizontal forecast error correlations are anisotropic. The horizontal forecast error correlations are anisotropic to account for nonuniform coverage of assimilated observations. The correlation length is the longest in the zonal direction in the tropics where data are sparse. This correlation model accounts for the anisotropy resulting from the non-uniform distribution of observations that are assimilated in the ozone system. The vertical forecast error correlations are modeled using a function that is zero for points separated by more than five model levels (Gaspari and Cohn 1999). Computational savings in the statistical analysis algorithm are obtained through the use of this compactly supported error correlation model.

### ***Validation of GEOS ozone DAS***

The validation results for the ozone system that are presented here are from two assimilation experiments: from January to September of 1998 and from November to December of 1999. They are in agreement with and extend the validation results for winter 1992 given by Štajner *et al.* (1999a).

One measure of the quality of the assimilation is how well the system forecast and observations agree before they are blended together. The daily root-mean-square (RMS) difference between the total column ozone forecast and TOMS total column ozone observations is approximately 11 Dobson units or 3.6% in 1998 (Fig. 1) and about 10 Dobson units in 1999. A sharp drop in this RMS occurs over first several days, as the ozone field adjusts from the initial condition to

incorporate assimilated observations. The maximum in March corresponds to the increased dynamical activity in the Northern hemisphere. It is followed by a gradual decrease resulting in return to January levels in July. The difference between forecast and observations consists of the forecast model and TOMS errors. McPeters *et al.* (1998) characterized errors in TOMS: the random part of approximately 2%, and a time invariant bias of less than 3%. Thus the total error in TOMS is almost identical to the RMS in Fig. 1 indicating an accurate forecast. A comparison of analyzed profiles with SBUV observations between 50 and 2 hPa reveals the global root-mean-square difference of less than 15%. This is comparable to the independently reported SBUV errors (Bhartia *et al.* 1996).

Another step in validation is comparison with independent data types that are not assimilated in the system. Three external types of observations are used here. Independent profile measurements with vertical resolution better than 2 km are available from the Halogen Occultation Experiment (HALOE) (Bruhl *et al.* 1996). The mean HALOE profile for January 1998 is shown in Figure 2, together with the mean of analysis profiles nearest to HALOE measurement times and locations. In January 1998, the RMS difference between HALOE and analysis fields is better than 20% and mean difference is better than 6.5% of the HALOE mean between 30 hPa and 1 hPa. In July 1998, after assimilation continued for six more months, the differences between HALOE and analysis are smaller than in January between these pressure levels. Bruhl *et al.* (1996) found that between these pressure levels HALOE measurements agree within 5% with other ozone measurements (from ozone sondes, lidars, balloons, rocket sondes and other satellites). This establishes that the assimilated fields are of quality comparable to HALOE and other profile measurements.

Independent measurements of tropospheric and lower to middle stratospheric profiles are available from WMO ozone sondes. The RMS difference between WMO ozone sonde measurements and analyzed ozone profiles relative to the mean of sonde measurements is shown in Fig. 3. The solid curve corresponds to the beginning of assimilation in January and the dashed curve to its end in September of 1998. The RMS in January generally increases with pressure between 10 and 850 hPa. It is less than 20% for pressure lower than 50 hPa, about 40% at 100 hPa, increases to 60% at 300 hPa and further at 850 hPa. Compared to January, the RMS in September is lower at 850 hPa and higher at 150 hPa. Separate comparisons with sondes in low, middle and high latitudes showed that this increase in the RMS difference between sondes and analysis occurs near the average tropopause height in each region. The behavior of this RMS for winter 1992 is similar (Štajner *al.* 1999b). No accumulation of errors was found in the free troposphere, away from the tropopause.

An example of validation covering all nine months in 1998 is given in Fig. 4. Monthly statistics at 20 hPa were computed: mean of the ozone sonde measurements, mean ozone analysis and their RMS difference. All these statistics are stable in time and there is no accumulation of errors. On the contrary, the RMS difference decreases in March and remains stable on this lower level.

The Polar Ozone and Aerosol Measurement (POAM) III data was compared with HALOE and ozone sondes by Lucke *et al.* (1999). The POAM and HALOE means agree within about 5% between 15 and 55 km altitude. A comparison of POAM with sondes shows agreement of the

means within 5%. We use the independent POAM data for validation of the analyzed ozone data for November and December 1999. The profiles used in this comparison were measured in the winter hemisphere between latitudes of 63.5 N and 65 N. The mean of 278 POAM profiles is shown in Fig. 5. The analysis profiles were interpolated from pressure to height levels using an approximate relationship between them with a constant scale height of 6.6 km. The resulting analysis mean (also shown in Fig. 5) agrees with the POAM mean in the profile shape. However, analysis ozone is higher than POAM between about 23 and 40 km. Note that some of this difference might be due to the POAM data. Lucke *et al.* (1999) found that the mean of POAM is lower than sonde mean between 25 and 30 km for the station in the winter hemisphere in their comparison.

We have shown a good agreement between analysis fields and independent profile observations. Using the comparison with the input data types, we have shown that the forecast model faithfully propagates the information for 24 hours. During a nine months long assimilation the quality of ozone fields is mostly stable. Middle and upper stratospheric and tropospheric profiles slightly improve. The quality of total ozone is constant except for the maximum in error that occurs during northern hemisphere spring. There is an increase in error around the tropopause.

## References

Bhartia, P. K., R. D. McPeters, C. L. Mateer, L. E. Flynn, and C. Wellemeyer, 1996: Algorithm for the estimation of vertical ozone profile from the backscattered ultraviolet (BUV) technique, *J. Geophys. Res.*, **101**, 18793-18806.

Bruhl, C., S. R. Drayson, J. M. Russell III, P. J. Crutzen, J. M. McInerney, P. N. Purcell, H. Claude, H. Gernandt, T. J. McGee, I. S. McDermid, and M. R. Gunson, 1996: Halogen Occultation Experiment ozone channel validation, *J. Geophys. Res.*, **101**, 10217-10240.

Cohn S. E., A. da Silva, J. Guo, M. Sienkiewicz and D. Lamich, 1998: Assessing the Effects of Data Selection with the DAO Physical-space Statistical Analysis System, *Mon. Wea. Rev.*, **126**, 2913-2926.

Gaspari, G. and S. E. Cohn, 1999: Construction of correlation functions in two and three dimensions, *Q. J. R. Meteorol. Soc.*, **125**, 723-757.

Lin, S.-J. and R. B. Rood, 1996: Multidimensional Flux-Form Semi-Lagrangian Transport Schemes, *Mon. Wea. Rev.*, **124**, 2046-2070.

Lucke R. L., D. R. Korwan, R. M. Bevilacqua, J. S. Hornstein, E. P. Shettle, D. T. Chen, M. Daehler, J. D. Lumpe, M. D. Fromm, D. Debrebian, B. Neff, M. Squire, G. Konig-Langlo, J. Davies, 1999: The Polar Ozone and Aerosol Measurement (POAM) III instrument and early validation results, *J. Geophys. Res.*, **104**, 18785-18799.

McPeters, R. D., P. K. Bhartia, A. J. Krueger, J. R. Herman, C. G. Wellemeyer, C. J. Seftor, G. Jaross, O. Torres, L. Moy, G. Labow, W. Byerly, S. L. Taylor, T. Swissler, R. P. Cebula, 1998: *Earth Probe Total Ozone Mapping Spectrometer (TOMS) Data Products User's Guide*, NASA

Technical Publication 1998-206895, National Aeronautical and Space Administration, Washington DC.

Riishøjgaard, L. P., I. Štajner and G.-P. Lou, 1999: The GEOS Ozone Data Assimilation System, *Adv. Space Res.*, in press. Available from [http://dao.gsfc.nasa.gov/DAO\\_people/ivanka/](http://dao.gsfc.nasa.gov/DAO_people/ivanka/)

Štajner, I., L. P. Riishøjgaard, and R. B. Rood, 1999a: The GEOS ozone data assimilation system: specification of error statistics, *submitted*.

Štajner, I., L. P. Riishøjgaard, and R. B. Rood, 1999b: The impact of withholding observations from TOMS or SBUV instruments on the GEOS ozone data assimilation system, *Proceedings of the 10th Conference on Satellite Meteorology and Oceanography*, Long Beach, California, January 2000. Available from [http://dao.gsfc.nasa.gov/DAO\\_people/ivanka/](http://dao.gsfc.nasa.gov/DAO_people/ivanka/)

*Figures*

# Daily global RMS of TOMS observed-minus-forecast residuals

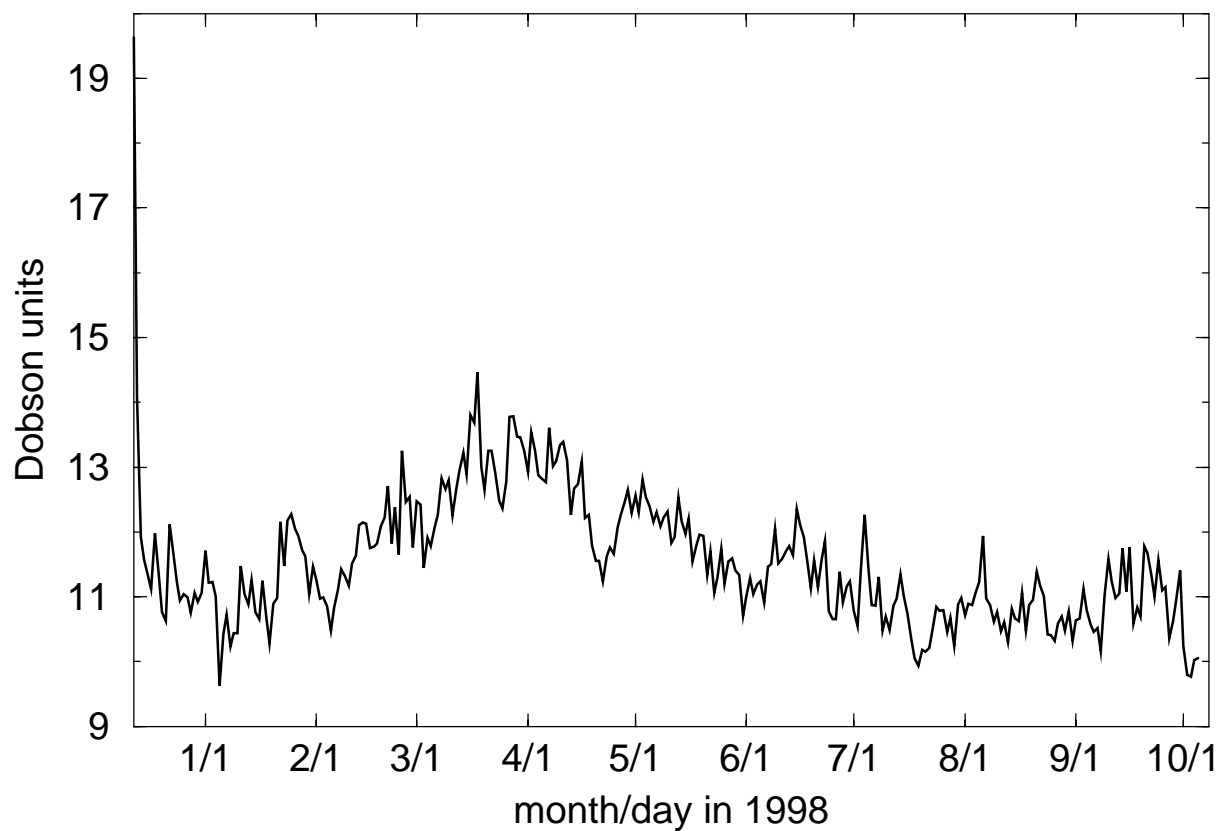


**Figure 1:** The daily root-mean-square (RMS) difference between the total column ozone forecast and TOMS total column ozone observations from December 13, 1997 to October 6, 1998 is shown.

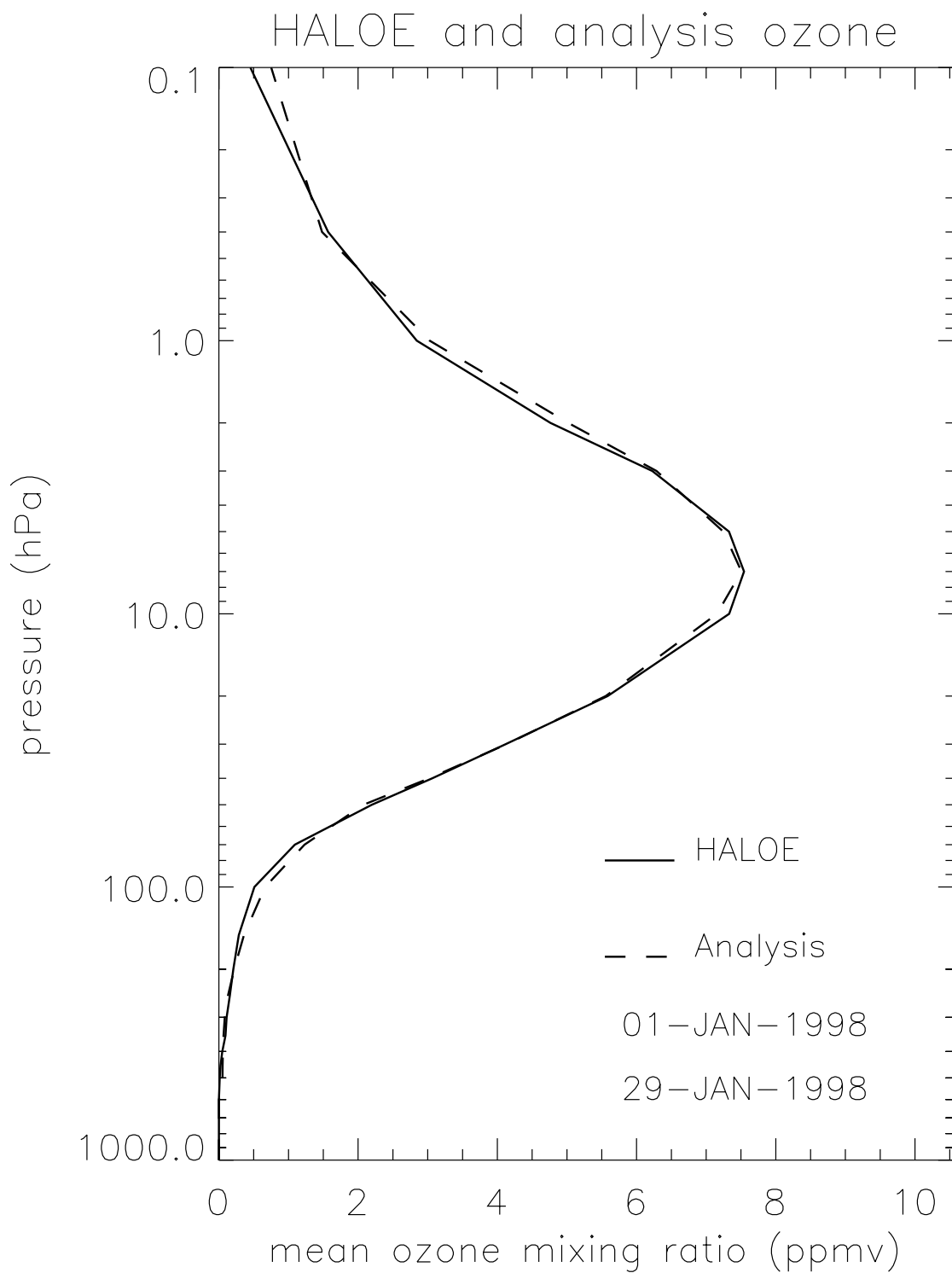


**Figure 2:** The means of independent HALOE and analysis ozone profiles are shown. The HALOE measured 551 profiles at sunset and sunrise between the latitudes of 72S and 47N.

## RMS difference between sondes and analysis relative to mean of sonde observations

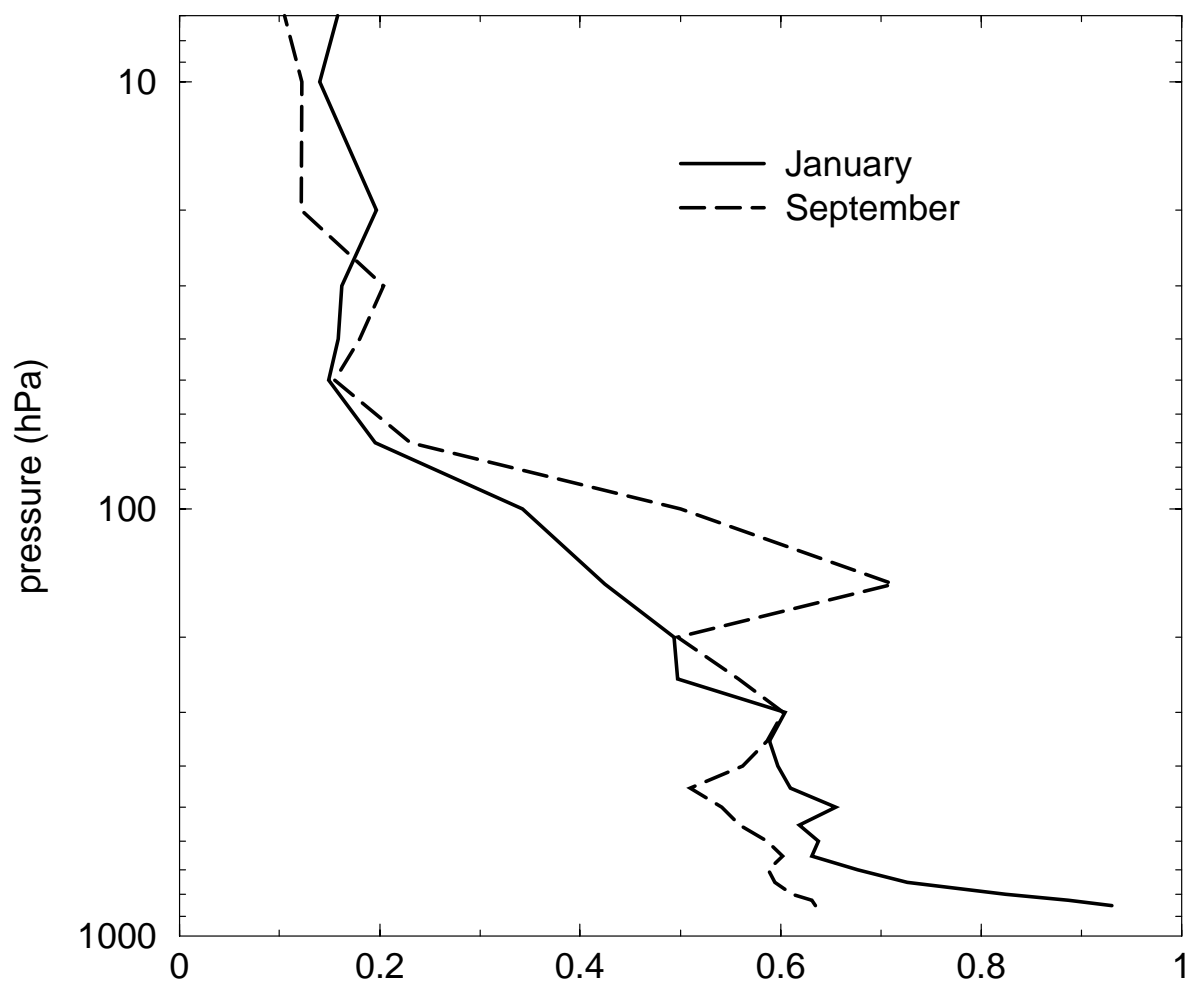


**Figure 3:** The RMS difference between independent ozonesonde measurements and ozone analysis is shown for January (solid line) and September (dashed line) 1998.



## Monthly statistics at 20 hPa

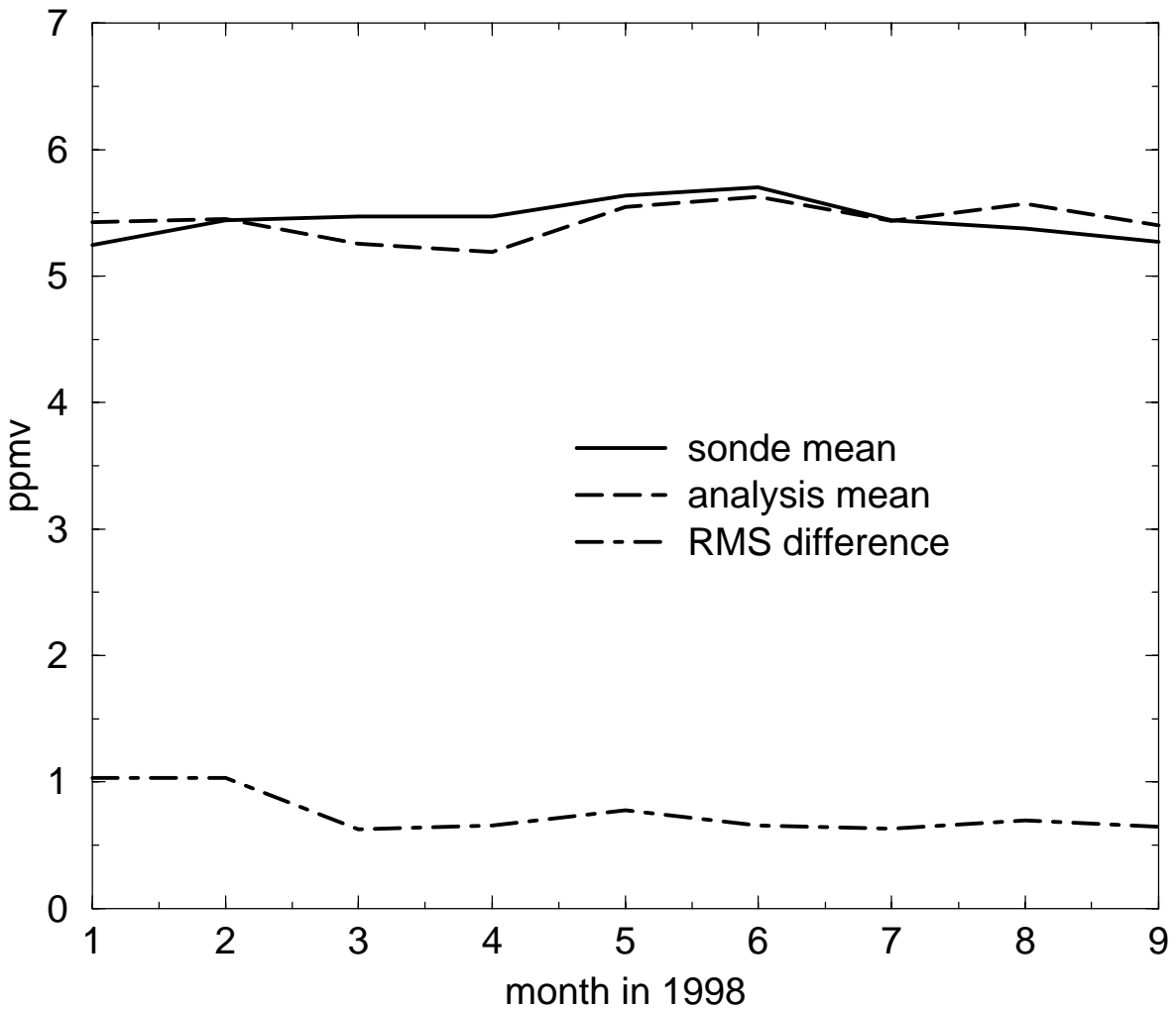


**Figure 4:** For nine months in 1998 monthly quantities at 20 hPa are shown: sonde mean (solid line), analysis mean (dashed line), and the RMS difference between sondes and analysis. The differences between independent sonde measurements and the ozone analysis are stable in time, after a decrease in the RMS in March.

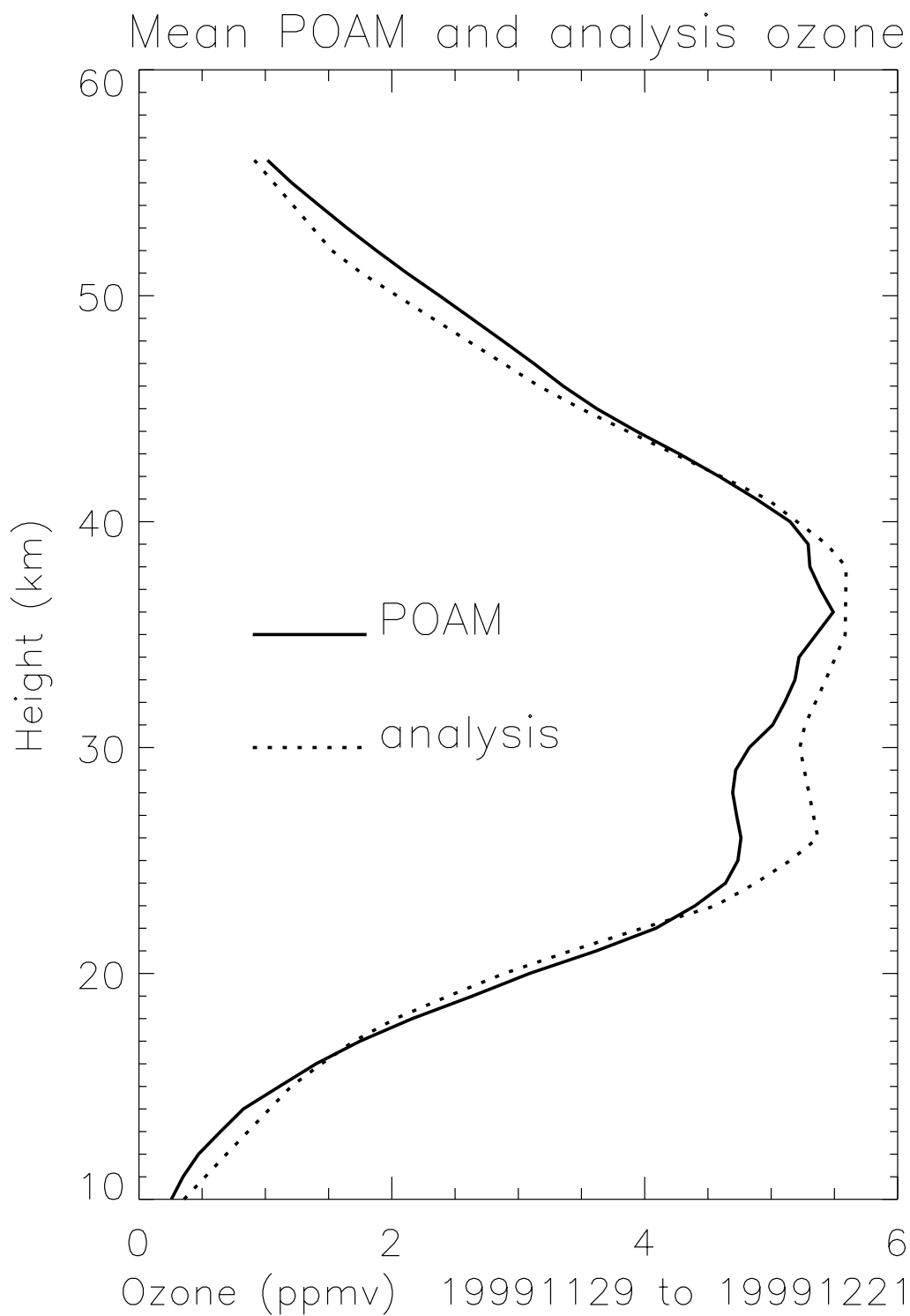


**Figure 5:** Mean POAM and analysis profiles from November 29 to December 21, 1999 are shown. The analysis profiles were interpolated from pressure to height levels using a constant scale height of 6.6 km. The POAM measurements were made between latitudes of 63.5N and 65N.